

Effect of Sintering Temperatures on Microstructural Changes and Phase Transformation of Nearly Equiatomic Microporous NiTi Alloy Produced by Metal Injection Moulding

*Mashitah Maso'od, Muhammad Hussain Ismail**
Centre of Advanced Materials Research, Industrial Metallurgy Research Group, Faculty of Mechanical Engineering, Universiti Teknologi MARA (UiTM), 40450 Shah Alam, Selangor, Malaysia

Rosliza Razali, Istiqamah Subuki
Faculty of Chemical Engineering, Universiti Teknologi MARA (UiTM), 40450 Shah Alam, Selangor, Malaysia

**hussain305@salam.edu.uitm.my*

ABSTRACT

In this present work, NiTi alloy were produced by metal injection moulding using elemental powders of Ni and Ti. The binder system comprised of palm stearin (PS). Two compositions of NiTi alloy were investigated; 50 at.% Ni, and 50.8 at.% Ni. Injection moulding was carried at 130°C, followed by solvent extraction using heptane as the solution. In a high vacuum furnace, the samples were thermally debound at 500°C and subsequently sintered at three different temperatures; 1050, 1100 and 1150 °C. All sintered samples were charateried by XRD and SEM for phase and microstructural analysis, respectively. Reversible phase transformation temperatures (PTTs) of austenite to martensite was determined by DSC analysis. The results showed that B2 (Austenite) and B19' were the main phases identified while minor phases consist of minimal fractions of Ti-rich phases (NiTi₂/Ni₂Ti₄O_x) and Ni-

rich phases (Ni_3Ti and Ni_4Ti_3). As composition of Ni content increased, the reversible martensite to austenite PTTs became wider while enthalpy for phase transition decreased. The FESEM microstructural analysis defined the formation different phases of atomic mass from dissimilar grey scale contrast. Brightest region assumed to be Ni_4Ti_3 formation and vice versa indicated Ti-rich phases ($NiTi_2/Ni_2Ti_4O_x$).

Keywords: NiTi Alloy, Metal Injection Moulding (MIM), sintering, phase transformation

Introduction

NiTi alloys is known for its outstanding characteristics compared to others alloy, which are, shape memory effect (SME), pseudoelasticity and high damping properties [1,2]. Since it was introduced, NiTi alloy had captivated many interest from various application especially in biomedical industry. Until present, there are few medical devices that had been implemented based on NiTi alloy material including orthodontic wires and intravascular stents that utilized the superelasticity behaviour [3]. Nowadays, the current interest of NiTi alloy besides its unique characteristics is the potential of the material toward porous structure implant [1]. Porous implant is desirable due to the ability in minimizing the 'stress shielding effect' associated by the mismatch of modulus between the bone tissue and the implant [4]. Osseointegration is another prime reason for porous implant as it important for an implant to fully integrate with surrounding bone to prevent loosening of prosthesis onward [6]. Hence, the process of implanting can be expedited along with the recovery duration while reducing the agony to the patient [7]. The ideal criteria recommended for porous titanium alloy as biomedical implant including porosity level ranging 30-80% with sizes between 100-600 μm , low Young's modulus and ≥ 100 MPa strength at 2% strain [7,8].

Bram et. al. mentioned that powder metallurgy (PM) is a favourable method in producing materials, such as NiTi since it is complicated to be fabricated through machining by conventional ways [9]. Elahinia et. al. summarized the manufacturing method of NiTi alloy by PM into two categories; conventional processes and additive manufacturing. Conventional sintering, hot isostatic pressing, self-propagating temperature and injection moulding are among the conventional techniques [10,11]. Metal injection moulding (MIM) is the most promising and effective mechanism in producing dense and porous NiTi alloy [9,12].

Metal injection moulding (MIM) is desirable since it can fabricate complex shape with minimal waste material. The main processes in MIM are mixing of powders and binder, injection moulding, debinding and lastly sintering [13,14]. In his publication, Bram et. al. conclude a baseline for Ti-

MIM process, indicating the specific time, temperature and such for each of the process for better optimization during injection molding [14]. There are few publications that successfully fabricated porous NiTi alloy, varying in term of elemental powders selection, binder composition and processes [7, 8, 11, 15]. Guoxin et. al. successfully fabricated porous NiTi alloy with 75 vol% porosity with almost three dimensionally interconnected [15]. Another work by Ismail, 2012, using water soluble binder system managed to fabricate porosity of 39-45% with pore size of 110 μm [12]. The following year, Chen et. al. was the first that introduced environmentally friendly binder, agar based in MIM to minimize the formation of impurities for the end product [8].

Ismail et. al. performed similar study in evaluating effect of sintering temperatures to porous NiTi alloy using four temperatures; 950°C, 1050°C, 1150°C and 1250°C. It can be concluded that temperatures above 1050°C and below 1250°C is the good range of sintering for appropriate mechanical properties [12]. In this present study, porous NiTi alloy was produced using elemental powders of Ni and Ti, mixed together with Palm Stearin (PS) and Polyethylene (PE) binders by MIM. This research focusing on the effect of sintering temperatures from 1050°C, 1100°C and 1150°C on the microstructural changes and phase transformation. Sintering is important as it determine the desired shape, size and quality of final product from green part [16].

Methodology

Metal Powder and Binder Characterization

Ni and Ti elemental powders used for the research were supplied by TLS Technik spezialpulver GmbH & Co, Germany and Sandvick Osprey, United Kingdom. The particle size of as-received powders were measured by Mastersizer 2000, Malvern Instrument and summarized in Table 1 including the packing density.

Table 1: Particle size distribution of elemental powders

Powder	Particle Size (μm)			Packing density (g/cm^3)		
	d_{10}	d_{50}	d_{90}	Apparent	Tap	Pycno
Nickel	3.911	7.872	14.991	3.73	5.11	8.7486
Titanium	5.587	10.856	19.786	1.53	2.56	4.4713

The method of determining the packing density were done in three various method; apparent, tap and pycnometer. Apparent and tap densities were measured following MPIF Standards 43 and 46 (MPIF, 1998), while,

theoretical densities were determined by pycnometer based on specific standard in MPIF Standard 35 that using Accupyc® under a flow of helium gas. Rigaku X-Ray Diffractometer (XRD) was used to identify the phases for the as-received powders of Ni and Ti.

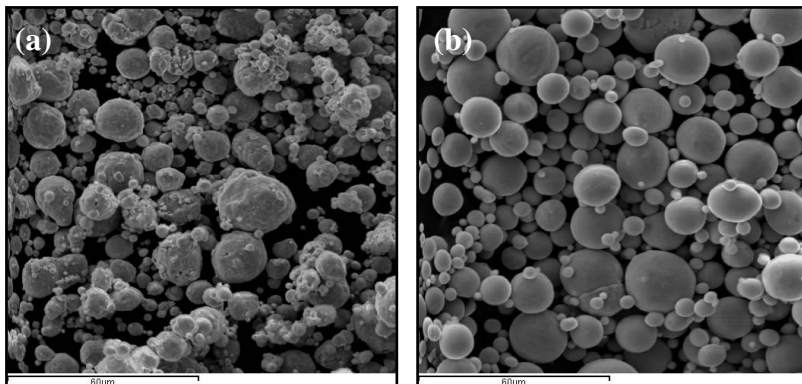


Figure 1: SEM Images of (a) Nickel (b) Titanium

Sample Preparation

In present study, two nearly equiatomic compositions of elemental powders of Ni and Ti were used; 50.0 at.% Ni/ 50.0 at.% Ti and 50.8 at.% Ni/ 49.2 at.%. Pulverisette 6, Planetary Mill was used to mix each of the composition at duration of 4 hours with ball-to-powder ratio of 2:1 for consistent distribution of as-mixed powders. Slow rotation was performed to avoid changes of powder surface during the blending. The binder selection consist of Palm Stearin (PS) and Polyethylene (PE) with percentage weight ratio of PS/PE at 60/40. Powder loadings of as-mixed powders used was 65.5 vol.%, mixed together with the binder composition. Internal mixer HAAKE Rheomix was used for mixing process at temperature of 160°C with rotational speed of 50 rpm for 2h until homogenous mixture achieved. The feedstock was manually chopped using pallet knife after mixing process completed and being cooled at room temperature.

Injection molding was conducted using bench-top injection moulding machine. The components of the machine consist of vertical injection structure, a plunger, melting chamber and heater with temperature feedback system as shown in schematic diagram, Figure 2. Before injection, the machine was thoroughly cleaned with acetone solution especially on parts that directly contact with feedstock; nozzle, barrel and hopper to prevent any contamination during the process. Moulding temperature was set in range between 110 to 150°C with pressure of 0.8 MPa. In this research, the samples were prepared according to ASTM 638-type V standard.

The tensile-shaped model green parts were dissolved in n-heptanes solution for 5 hours at temperature of 60°C to remove the palm stearin binder. Then, in order to remove the heptane solution, the leached samples were dried off in oven for 4 to 5 hours at temperature between 45-50°C. Thermal debinding was done at temperature of 500°C at ramp rate 3°C/min for 1 hours where PE was removed completely followed by sintering process in the same vacuum furnace using High Vacuum Tungsten Furnace. At ramp rate 10°C/min, the temperature for sintering was continued until reached required temperatures of 1050, 1100 and 1150°C followed at 1hour accompanied by furnace cooling at natural rate as no power was supplied.

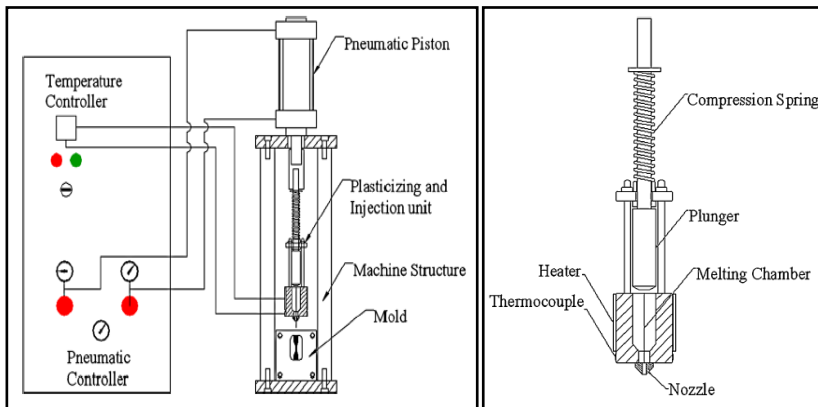


Figure 2: (a) Schematic of custom-made vertical injection moulding machine
(b) plunger drawing with heater and thermocouple [17]

Characterization of as-sintered NiTi alloy

The characterization of as-sintered NiTi alloy is focusing on microstructural analysis, qualitative phase analysis by XRD and Differential Scanning Calorimetry (DSC). For microstructural observation, as-sintered samples were cut using diamond cutter, grinded, polished and lastly, etched by Kalling's solution before observed under optical microscope. DSC was done in determining the reversible phase transformation temperature using Mattler Toledo of Differential Scanning Calorimetry Model 700. In determining DSC measurement of as-sintered NiTi alloy, around 10-20 mg of weight sample was required as sample was being crushed first. The crushed sample was placed inside the crucible where it was being analysed at heating and cooling rates of 10°C min⁻¹ under nitrogen atmosphere (20mL/min) in a temperature range of -50°C to 200°C.

Results and Discussion

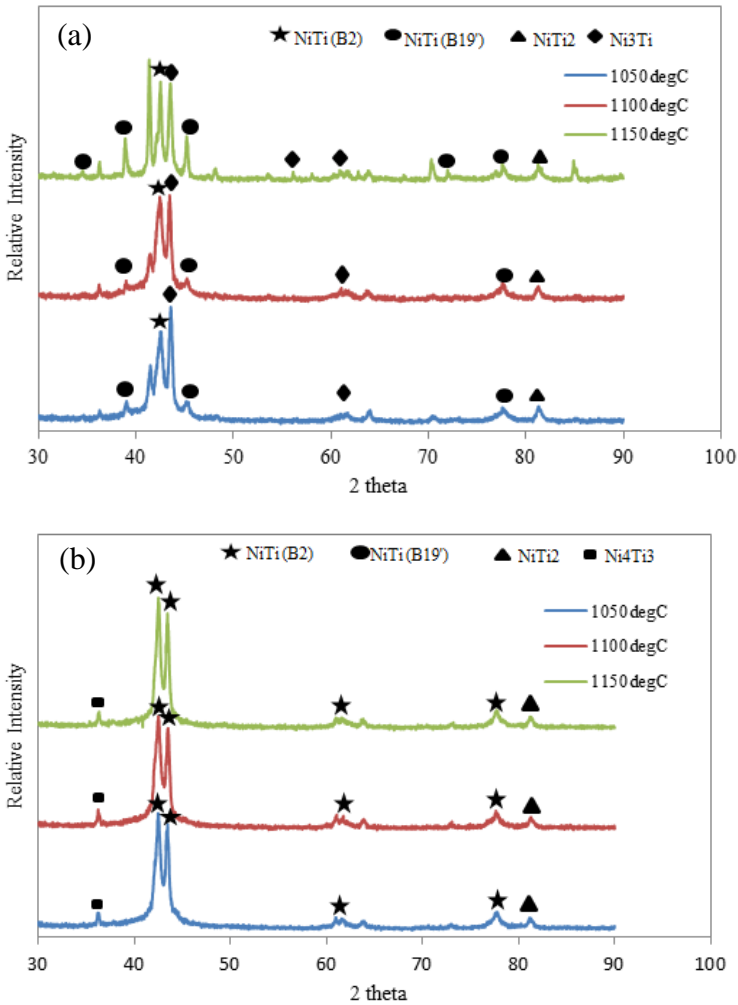


Figure 3: XRD patterns of NiTi sintered parts at different composition a) 50 at.% Ni and b) 50.8 at.% Ni and sintering temperature (1050,1100 and 1150°C)

XRD Analysis

XRD patterns of sintered NiTi with different ratio can be observed in Figure 3. The samples were observed at two different composition at (a) 50.0 at.% Ni and (b) 50.8 at.% Ni, sintered at three different temperatures of 1050°C,

1100°C and 1150°C. Based on observation for each composition, the major formation is controlled by intermetallic phases of NiTi; (B2) Austenitic and (B19') Martensitic resulted from complete inter-diffusion during sintering between elemental Ni and Ti powders. For 50.0 at.% Ni composition, the formation of secondary phases of NiTi₂ and NiTi₃ are shown, in which may affected the mechanical strength due to brittleness of that phase. However, at composition 50.8 at.% Ni, NiTi (B2) phase was determined along with fraction of B19' phase, assuming that diffusion process during sintering was completed between Ni and Ti powders.

Microstructural Analysis by SEM

Field Emission Scanning Electron Microscopy (FESEM) under back scattered (BS) mode was done in determining the phases distinguished during XRD analysis. Microstructures of two different compositions; a) 50.0 at.% Ni and b) 50.8 at.% Ni were presented in Figure 4. There are three different grey scale contrast can observed showing different intensity atomic mass for different phases, identical to composition medium gray matrix phase of NiTi [18]. The lighter needle-like structure which disappears when heated represent to martensite and the darker gray phase is believed to be the Ti-rich phase owing to lower atomic mass of the phase which is NiTi₂. The Ni-rich phase, particularly Ni₄Ti₃ with higher atomic mass was observed as the brightest gray-scale contrast and the structure shows almost similar characteristics with the B19' phase. The traces of oxygen and carbon were also observed when it was further analysed by the EDX, minor phases of Ni₂Ti₄O_x and TiC indicating greater tendency of impurities had been introduced, mainly originated from the binder residue.

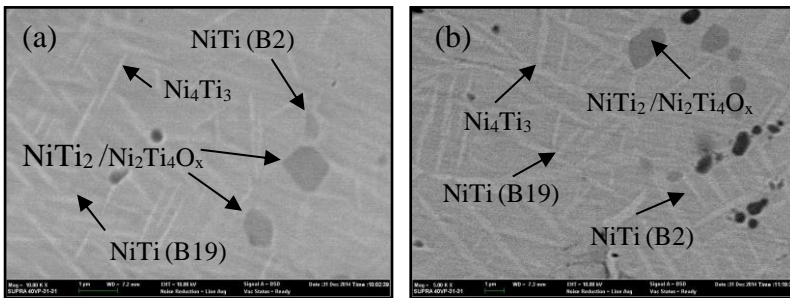


Figure 4: Back-scattered SEM of the as-polished sample at different composition (a) 50.0 at.% Ni and (b) 50.8 at.% Ni

Phase Transformation Analysis by DSC

The phase transformation of as-sintered NiTi alloy can be observed based on the temperatures in Table 2 and plotted graph in Figure 5 and 6. The main purpose of DSC is to indicate the approximate reversible martensite (B19')

and austenite (B2) during heating and cooling. Based on the PTTs and enthalpies in Table 2, the reversible transformation during heating and cooling were indicated, proving that Ni and Ti powders were significantly diffused during sintering, as NiTi phase was dominant during the development of transient liquid phase. At 50.8 at% Ni, the austenite finish, A_f are lower compared to 50.0 at% Ni at three different temperatures where the transformation peak reduced and broader due to the transition of R-phase during B19' to B2 transformation.

The phase transformation temperatures (PTTs) behaviour can be observed in Figure 5 for heating and Figure 6 for cooling. The transformation peaks at each composition during heating show that clear single peak of reversible austenitic to martensitic at lowest Ni composition while Ni-rich compositions multiple peaks appeared due to the two step transformation between B2 to R-phase to B19'.

Table 2 : Phase transformation temperatures (PTTs) of the as-sintered NiTi samples at different composition

(a) 50.0 at. % Ni / 50.0 at. % Ti

at %Ni	Enthalpy, ΔH (J/g)		Transformation temperature ($^{\circ}C$)					
	Heating	Cooling	As	Ap	Af	Ms	Mp	Mf
1050	-8.23	6.68	59.34	88.17	104.81	84.09	59.22	37.32
1100	-6.15	7.40	-6.37	61.96	92.00	62.63	29.20	-11.16
1150	-6.66	5.99	37.65	68.34	95.30	65.54	41.04	14.74

(b) 50.8 at. % Ni/ 49.2 at. % Ti

at %Ni	Enthalpy, ΔH (J/g)		Transformation temperature ($^{\circ}C$)					
	Heating	Cooling	As	Ap	Af	Ms	Mp	Mf
1050	-3.34	1.08	-12.79	5.29	39.21	32.34	-0.80	-14.31
1100	-4.54	1.68	-19.64	7.30	46.47	43.97	3.20	-19.34
1150	-5.40	2.13	-15.20	18.47	55.35	55.46	32.36	-12.28

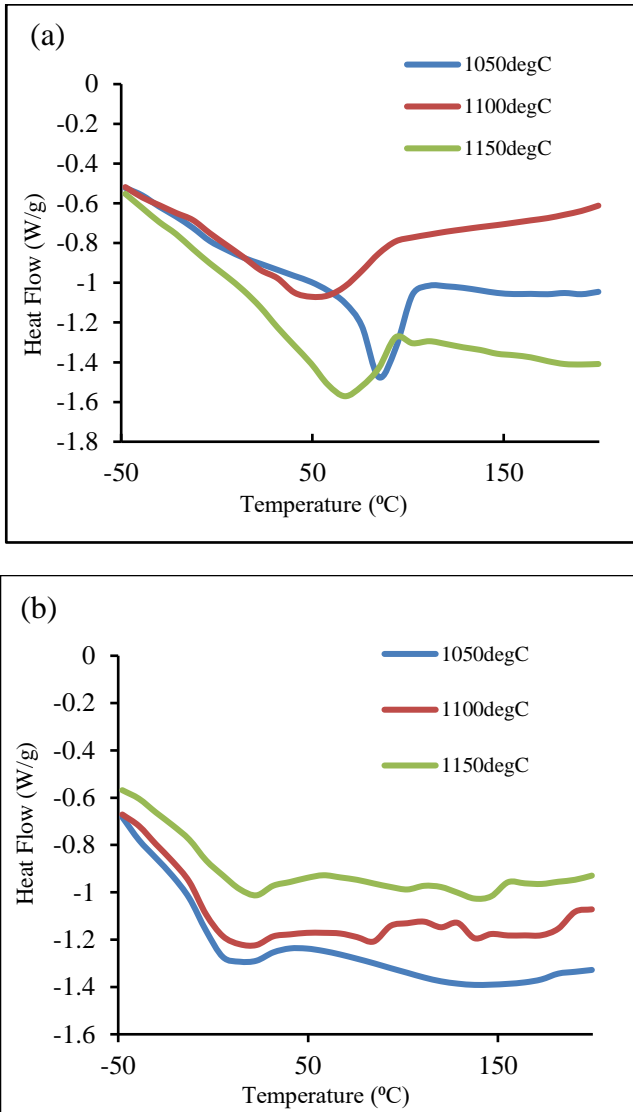


Figure 5: DSC curves for sample (a) 50.0 at.% Ni and (b) 50.8 at.% Ni during heating

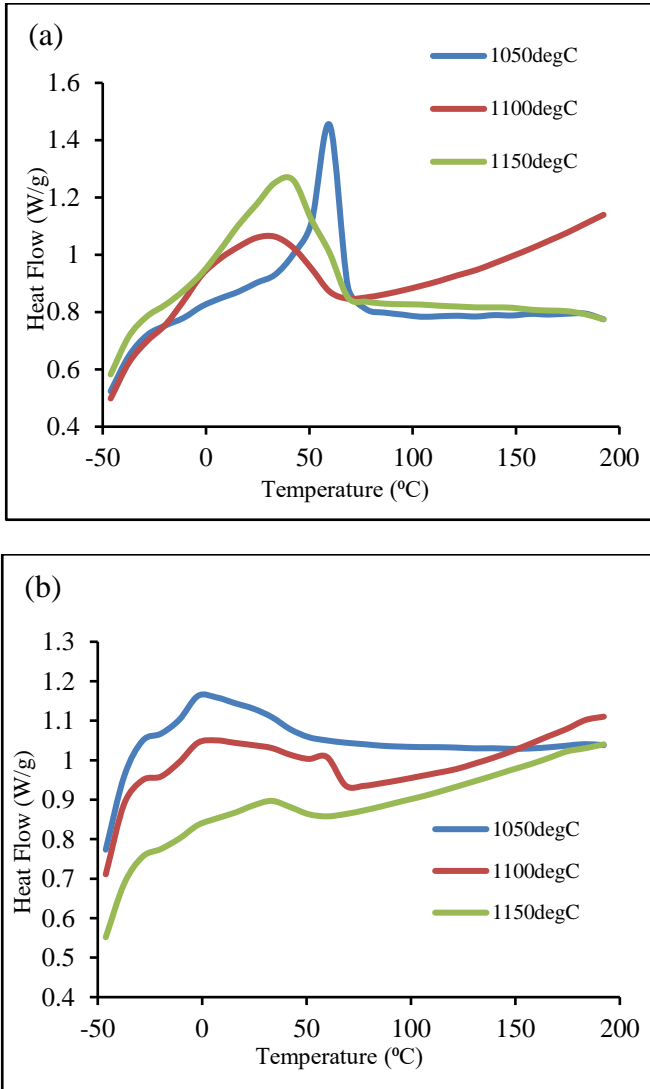


Figure 6: DSC curves for sample (a) 50.0 at.% Ni, (b) 50.4 at.% Ni and (c) 50.8 at.% Ni during cooling

Conclusion

In conclusion, NiTi alloy with combination of elemental powders of Ni and Ti with palm stearin (PS) as the binder was successfully produced with MIM

using optimum temperature of 130°C. NiTi (B2) Austenitic and (B19') Martensitic were clearly defined as the dominant phases under XRD analysis done with minor formation of Ti-rich phases ($\text{NiTi}_2/\text{Ni}_2\text{Ti}_4\text{O}_x$) and Ni-rich phases (Ni_3Ti and Ni_4Ti_3). During SEM analysis, all of the phases identified as grey-scale contrast defined different atomic mass of phases. Needle-like structure, Ni_4Ti_3 phase identified as the brightest contrast where darkest contrast indicated the Ti-rich phases ($\text{NiTi}_2/\text{Ni}_2\text{Ti}_4\text{O}_x$). The wider reversible transformation from martensite to austenite with the decreasing values of enthalpy showed that increasing amount of Ni content.

Acknowledgement

The authors would like to thank Ministry of Education (MOE) and Universiti Teknologi MARA for awarding the listed grants in supporting and financing further development of NiTi alloy by MIM from 2012 until present.

1. FRGS Grant (2012-2015) : [RMI/FRGS 5/3(38/2012) – Advanced NiTi Intermetallic Compounds Superior Shape Memory Behaviour]
2. RACE Grant (2012-2015) : [600-RMI/RACE 16/6/2(5/2012) – The Influence Of Locally Binder System And Processing Conditions On Nearly Equiatomic NiTi Alloys]
3. FRGS Grant (2015-present) : [600-RMI/FRGS 5/3(72/2015) - Titanium Hydride Superior Shape Memory Intermetallic Nickel titanium Alloy]

References

- [1] A. Nouri, "Titanium foam scaffolds for dental applications", Elsevier-Woodhead Publishing, pp. 131-160, 2017.
- [2] Z. Abdullah, R. Razali, I. Subuki, M.A. Omar and M.H. Ismail, "An Overview of Powder Metallurgy (PM) Method for Porous Nickel Titanium Shape Memory Alloy (SMA)", *Advanced Materials Research* Vol. 1133. Pp. 269-274, 2016.
- [3] O. Prymak, D. Bogdanski, M. Koller, S.A. Esenwein, G. Muhr, F. Beckmann, T. Donath, M. Assad and M. Epple, "Morphological characterization and in vitro biocompatibility of a porous nickel-titanium alloy", *Biomaterials* 26, pp. 5801-5807, 2005.
- [4] C.L. Jian, L.I. Ting, L.Y. Min, H. Hao and H.Y. Hua, "Porous titanium implants fabricated by metal injection molding", *Transaction of Nonferrous Metals Society of China*, pp. 1174-1179, 2009.
- [5] A.D. Pogrebnyak, A.S. Krivets, Z.K. Shaimardanov, B.V. Syrnev, S.V. Plotnikov and O.V. Maksakova, "Surface Properties, Technology of Fabrication and Prospects of Application of Medical Implants from Porous Titanium Obtained by Powder Metallurgy, International Conference on Nanomaterials : Application and Properties (NAP), 2016.

- [6] Q. Chen and G.A. Thouas, "Metallic implant biomaterials", *Materials Science and Engineering R* 87, pp. 1-57, 2015.
- [7] M.H. Ismail, R. Goodall, H.A. Davies and Iain Todd, "Formation of microporous NiTi by transient liquid phase sintering of elemental powders", *Materials Science and Engineering C* 32, pp. 1480-1485, 2012.
- [8] G. Chen, P. Cao, G. Wen, N. Edmonds and Y. Li, "Using an agar-agar based binder to produce porous NiTi alloys by metal injection moulding", *Intermetallics* 37, pp. 92-99, 2013.
- [9] M. Bram, "Applications of powder metallurgy in biomaterials", Woodhead Publishing Limited, 2013, pp. 520-554.
- [10] M.H. Elahinia, M. Hashemi, M. Tabesh and S.B. Bhaduri, "Manufacturing and processing of NiTi implants: A review", *Progress in Materials Science* 57, pp. 911-946, 2012.
- [11] M. Kohl, M. Bram, A. Moser, H.P. Buchkremer, T. Beck and D. Stover, "Characterization of porous, net shaped NiTi alloy regarding its damping and energy-absorbing capacity", *Materials science and Engineering A* 528, pp. 2454-2462, 2011.
- [12] M.H. Ismail, R. Goodall, H.A. Davies and Iain Todd, "Porous NiTi alloy by metal injection moulding/sintering of elemental powders: Effect of sintering temperature", *Materials Letter* 70, pp. 142-145, 2012.
- [13] R.M. German and A. Bose, "Injection Molding of Metals and Ceramics", Metal Powder Industries Federation, 1997.
- [14] R.M. German, "Progress in Titanium Metal Powder Injection Molding", *Materials*, pp. 3641-3662, 2013.
- [15] H. Guoxin, Z. Lixiang, F. Yunliang and L. Yanhong, "Fabrication of high porous NiTi shape memory alloy by metal injection molding", *Journal of Materials Processing Technology* 206, pp. 395-399, 2008.
- [16] R.M. German, "Powder Metallurgy & Particulate Materials Processing", Metal Powder Industries Federation, 2005.
- [17] M. azuddin, I.A. Choudhury and Z. Taha, "Development and performance evaluation of a low-cost custom-made vertical injection molding machine", *Journal of the Brazillian Society of Mechanical Sciences and Engineering*, 2014.
- [18] M. Bram, M. Bitzer, H.P. Buchkremer and D. Stover, "Reproducibility Study of NiTi Parts Made by Metal Injection Molding", *Journal of Materials Engineering and Performance* 21 (12), pp. 2701-2712, 2012.